Lawrence Berkeley National Laboratory

Title
Tailored laser pulse chirp to maintain optimum radiation pressure acceleration of ions

Permalink
https://escholarship.org/uc/item/9wm0x369

Journal
Physics of Plasmas, 26(2)

ISSN
1070-664X

Authors
Mackenroth, F
Bulanov, SS

Publication Date
2019-02-01

DOI
10.1063/1.5082604

Peer reviewed

Tailored laser pulse chirp to maintain optimum radiation pressure acceleration of ions EP

F. Mackenroth iD , and S. S. Bulanov

COLLECTIONS

EP   This paper was selected as an Editor's Pick

View Online

Export Citation

CrossMark

ARTICLES YOU MAY BE INTERESTED IN

Tailored laser pulse chirp to maintain optimum radiation pressure acceleration of ions

View Online   Export Citation   CrossMark

F. Mackenroth[1,a] (iD) and S. S. Bulanov[2]

AFFILIATIONS

[1]Max Planck Institute for the Physics of Complex Systems, Nöthnitzer Str. 38, 01187 Dresden, Germany
[2]BELLA Center, Lawrence Berkeley National Laboratory, 1 Cyclotron rd, Berkeley, California 94720, USA

[a]Electronic mail: mafelix@pks.mpg.de

ABSTRACT

Ion beams generated with ultra-intense laser-plasma accelerators hold promises to provide compact and affordable beams of relativistic ions. One of the most efficient acceleration setups was demonstrated to be direct acceleration by the laser's radiation pressure. Due to plasma instabilities developing in the ultra-thin foils required for radiation pressure acceleration, however, it is challenging to maintain stable acceleration over long distances. Recent studies demonstrated, on the other hand, that specially tailored laser pulses can shorten the required acceleration distance suppressing the onset of plasma instabilities. Here, we extend the concept of specific laser pulse shapes to the experimentally accessible parameter of a frequency chirp. We present a novel analysis of how a laser pulse chirp may be used to drive a foil target constantly maintaining optimal radiation pressure acceleration conditions for in dependence on the target's areal density and the laser's local field strength. Our results indicate that an appropriately frequency chirped laser pulse yields a significantly enhanced acceleration to higher energies and over longer distances suppressing the onset of plasma instabilities.

Published under license by AIP Publishing. https://doi.org/10.1063/1.5082604

I. INTRODUCTION

Beams of relativistic ions serve a wide range of applications from technical materials science, over medical applications to even fundamental studies of high energy physics. Some of these applications particularly benefit from short, dense ion beams, not necessarily of ultra-high energy.[1] Relativistic ion beams with the necessary high fluxes can be accelerated by high power lasers,[2] which have undergone considerable development over the past few decades,[3] with several facilities breaking the Petawatt (PW) barrier already operational,[4–7] under construction,[8,9] or in planning.[10–13] Consequently, the acceleration of ions to relativistic energies by high-power lasers is among the most intensely studied applications of such laser systems.[14–17]

As a result of this deep interest in laser-ion acceleration, there were several technical approaches proposed, to overcome the challenges of this application, such as the experimentally most widely studied target normal sheath acceleration (TNSA),[18–22] Coulomb explosion (CE),[23–29] hole boring (HB),[30,31] relativistic transparency (RT),[32–34] shock wave acceleration (SWA),[35] magnetic vortex acceleration (MVA),[36,37] standing wave schemes,[38,39] and several others to the highly efficient radiation

pressure acceleration (RPA).[40–43] In this latter regime, a thin solid density foil target is quickly ionized by the laser pulse to form a plasma, which reflects the incoming radiation and is consequently accelerated by the laser's radiation pressure. Furthermore, in the foil's rest frame the laser's frequency will appear down-shifted by a factor 2γ, where $\gamma = \epsilon/m_i$ is the foil's relativistic factor, with ϵ and m_i being the energy and mass of a single ion of the foil, respectively. It is thus apparent that for relativistic foil energies ($\gamma \gg 1$) the laser light's frequency is strongly reduced leading to almost complete transfer of laser energy to the foil. In this regime, due to the relativistic time dilation, the acceleration is maintained over a long time during which the foil almost co-propagates with the laser and constantly experiences its radiation pressure. It was shown that in an ideal setting this leads to the foil reaching an energy proportional to that of the accelerating laser pulse. We note that the development of instabilities[44] and the presence of other limiting factors, for example, laser group velocity and transverse target expansion,[45,46] limit the effectiveness of the RPA. However, it was shown recently that laser pulse tailoring and special target engineering might compensate these limiting factors.

The RPA was never experimentally tested in the ultra-relativistic regime due to the lack of necessary laser facilities; however, there are experimental indications that this scheme also works in the nonrelativistic regime.[42,43,47,48] It is less stable and less effective than in the ultra-relativistic regime, mainly because the foil reflectivity is no longer perfect, but depends complicatedly on the target areal density, as well as the laser's intensity, and frequency.[49-53] Including this non-trivial parameter dependence of the foil reflectivity in a one-dimensional model of its dynamics, it was demonstrated that the ion energies are optimized if for a foil of density and thickness n_e and l, respectively, moving with a momentum $p_0(t)$ at position $\boldsymbol{x}_0(t)$, corresponding to the single-particle energy $\varepsilon(t)$, by the radiation pressure of a laser pulse with electric field envelope $E(t, \boldsymbol{x})$ and frequency $\omega_0(t, \boldsymbol{x}) = 2\pi/\lambda_0(t, \boldsymbol{x})$, are related via the following optimum condition:[53]

$$a_0(t, \boldsymbol{x}_0(t)) = \gamma(t)\epsilon_0(t, \boldsymbol{x}_0(t)), \qquad (1)$$

where $a_0(t, \boldsymbol{x}) = |eE(t, \boldsymbol{x})|/(m_e\omega_0(t, \boldsymbol{x}))$ is the laser's dimensionless amplitude, the parameter $\epsilon_0(t, \boldsymbol{x}) = \pi(ln_e)/(\lambda_0(t, \boldsymbol{x})n_{cr}(t, \boldsymbol{x}))$, introduced in Ref. 49, is the target's areal density normalized to the product of the laser's wavelength λ_0 and the critical plasma density $n_{cr}(t, \boldsymbol{x}) = m_e\omega_0^2(t, \boldsymbol{x})/(4\pi e^2)$, where $e < 0$ and m_e are the electron charge and mass, respectively, and units with $c \equiv 1$ are used throughout. These equations are obtained for a monochromatic laser field, whence we have to assume the pulse chirp not to be too strong, such that the frequency change can be assumed to be adiabatic. The above condition's physical meaning states that the foil should be opaque to the laser radiation at all times, in order for the required reflection to be facilitated. On the other hand, the foil density must not be too high, in order to distribute the laser energy on as few particles as possible, ensuring that each individual particle experiences the largest possible energy gain. The condition (1) ensures the optimum compromise between these two trends. On the other hand, upon acceleration the foil becomes more and more opaque, as argued above, and hence the condition (1) changes over time. It was shown recently, however, how it can still be satisfied nonetheless throughout the whole acceleration process, if the laser is given an optimally tailored intensity profile.[53]

In this paper, we study how the optimum condition (1) can be optimized through a tailored frequency profile, instead. We are going to demonstrate that the changes of the reflectivity can be counteracted by a complicated frequency chirp of the driving laser pulse and derive a closed analytical form of the laser's required frequency dependence. We note that the problem of the laser chirp influence on the ion acceleration was addressed in a number of papers;[54-57] however, a systematic analytical treatment of this problem in the case of a thin foil RPA was missing.

II. THEORY

We begin by reformulating the optimum condition in terms of basic quantities as

$$|\mathcal{E}(t, \boldsymbol{x}_0)| = \gamma(t), \qquad (2)$$

where we introduced the scaled electric field $\mathcal{E}(t, \boldsymbol{x}_0) = E(t, \boldsymbol{x}_0)/E_{foil}$, where $E_{foil} := 2\pi|e|ln_e$ is the static, one-dimensional charge separation field of the foil. Next, we note that Eq. (2) is independent of the laser's frequency and thus infer that if the laser's electric field and frequency are independent the laser's frequency cancels out of the optimum condition and, provided the field amplitude is varied appropriately, Eq. (2) is fulfilled for all frequencies. The same conclusion can be drawn from Eq. (23) of Ref. 53, which is independent of the laser's frequency.

On the other hand, the frequency still does impact the acceleration process heavily, despite the fact that the optimum condition is independent of it. To demonstrate this, we turn to the foil's equation of motion[40]

$$\begin{aligned}
\frac{dp_0}{dt} &= \frac{K|E(t, \boldsymbol{x}_0)|^2}{4\pi ln_e} \frac{\sqrt{m_i^2 + p_0^2(t)} - p_0(t)}{\sqrt{m_i^2 + p_0^2(t)} + p_0(t)}, \\
\frac{dx_0^{\parallel}}{dt} &= \frac{p_0(t)}{\sqrt{m_i^2 + p_0^2(t)}}, \\
K &= 2|\rho|^2 + |\alpha|^2,
\end{aligned} \qquad (3)$$

where m_i is the mass of a single ion in the foil and ρ and α are the foil's reflection and absorption coefficient, respectively. We rewrite these equations to be expressed in the Lorentz invariant laser phase $\eta = \omega(t - x^{\parallel}(t))$, where again $x^{\parallel}(t)$ is the foil's position, to read

$$\begin{aligned}
\frac{dp_0}{d\eta} &= \frac{dp_0}{dt}\frac{dt}{d\eta} = \frac{|\rho(\eta)eE(\eta)|^2}{eE_{foil}} \frac{\sqrt{m_i^2 + p_0^2(\eta)}}{\sqrt{m_i^2 + p_0^2(\eta)} + p_0(\eta)}, \\
\frac{dt}{d\eta} &= \frac{\sqrt{m_i^2 + p_0^2(t)}}{\sqrt{m_i^2 + p_0^2(t)} - p_0(t)}.
\end{aligned} \qquad (4)$$

Separating the variables in this equation its general solution was found to be given by[40]

$$p_0(\eta) = \frac{1}{2}\left(h_0 + \mathcal{D} - \frac{m_i^2}{h_0 + \mathcal{D}}\right), \qquad (5)$$

$$h_0 := p_0(\eta_0) + \sqrt{p_0^2(\eta_0) + m_i^2}, \qquad (6)$$

$$\mathcal{D} := \int_{\eta_0}^{\eta} d\eta' \frac{|\rho(\eta')eE(\eta')|^2}{eE_{foil}}. \qquad (7)$$

We continue by rewriting condition (2) as a function of the phase-dependent momentum. We find that maintaining the optimum acceleration condition is ensured by the momentum fulfilling the condition

$$p_0^{opt}(\eta) = m_i\sqrt{\mathcal{E}^2(\eta) - 1}. \qquad (8)$$

We immediately conclude that this condition can only be satisfied for $|\mathcal{E}(\eta)| \geq 1$, whence we have to focus on this parameter regime in the following. We do so by having our analysis only start at the time instant η_0 defined by $|\mathcal{E}(\eta_0)| = 1$, where we assumed the foil to be at position $x(\eta_0) = 0$. In the following, we

assume the laser's intensity envelope to be given by a Gaussian of FWHM τ_L, modeled by a field envelope of the form $E(\eta) = E_{max} \exp[-2 \log(2)(\eta/\tau_L)^2]$, independently of the pulse chirp. We choose to fix the pulse envelope in accordance with the above reasoning, rather than, e.g., assuming a constant value of a_0 or laser intensity, as we wish to model a pulsed laser field of a given intensity profile, in agreement with experimental set-ups. Following this model, the threshold condition can be analytically solved to give the phase at which the laser reaches the threshold of the foil transparency

$$\eta_0 = \tau_L \sqrt{\frac{\log[\mathcal{E}_{max}]}{2 \log(2)}} \qquad (9)$$

such that the acceleration can only be optimized in the interval $\eta \in [-\eta_0, \eta_0]$. For all numerical examples studied below, we are going to consider the acceleration only in interval $\eta \in [-\eta_0, 0]$, however, as only during this interval the pulse envelope is rising allowing for an optimization of the acceleration through a pulse chirp, as argued below. Furthermore, here we consider a long laser pulse with $\tau_L = 10^2/\omega_0$. In order to test the improved ion acceleration regime, we numerically integrate Eq. (8) and compare it to a full numerical solution of the system (4). Furthermore, as we additionally wish to highlight the enhancement in the accelerated foil's position $x_0(\eta)$, we additionally solve its equation of motion

$$\frac{dx_0}{d\eta} = \frac{dx_0}{dt}\frac{dt}{d\eta} = \frac{p_0(t)}{\sqrt{m_i^2 + p_0^2(t)} - p_0(t)}, \qquad (10)$$

where we made use of the relativistic velocity relation $dx_0/dt = p_0(t)/\sqrt{m_i^2 + p_0^2(t)}$. In order to analyze the solutions of the respective equations of motion for the foil's momentum and position in the general as well as the optimized case we study a foil of density $n_e = 10^{24}$ cm$^{-3} \approx 574 n_{cr}$ for radiation of 800 nm wavelength, and thickness $l = 10$ nm accelerated by a moderately relativistic laser with intensity $I = 1.5 \times 10^{21}$W/cm^2. Furthermore, as we wish to analyze the efficiency enhancement as a function of space-time, we plot the foil's momentum in the laboratory frame as a function of its position by means of a parametric plot with the coordinates $(p_0(\eta)/m_i, \omega_0 x_0(\eta))$ (see Fig. 1). We find a significant enhancement of the foil's momentum, when accelerated according to the optimum condition p_0^{opt},
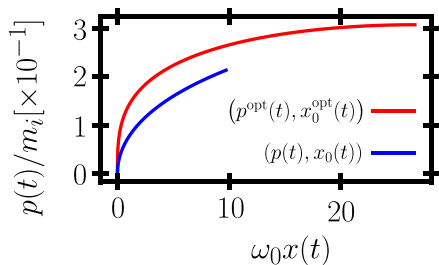

FIG. 1. Comparison of the foil's momentum in units of an accelerated ion's mass as a function of its position in units of wavelength in the general and the optimized case for the parameters given in the text.

derived from Eq. (8). We furthermore note that while we only consider the acceleration up to the phase value $\eta = 0$, the physical time extends to values larger than 0, for the simple reason that the non-trivial foil displacement $x_0(t)$ leads to a non-trivial relation between phase η and time $t = \eta + x_0(t)$. In this respect, we also note that since $p_0^{opt}(t) > p_0(t)$ it will be $x_0^{opt}(t) > x_0(t)$ as reflected in the fact that $\eta = 0$ is reached at larger displacements $x_0^{opt}(\eta)$ in the optimized regime. We note that this can be interpreted as the optimized case leading to a reduction of the acceleration length, i.e., the same ion energy can be reached over a smaller distance. This effect is clearly inferable from the fact that in the optimized case the ion momentum at any given foil position is higher than in the unoptimized case, indicating that the optimized pulse chirp needs significantly less distance to accelerate ions to a certain energy. Usually the acceleration length is limited by either the Rayleigh length or the transverse expansion of the target, or both. In the case of transversely flat-top (e.g., super-Gaussian) laser pulses, which are often suggested to be employed to produce quasi-mono energetic ion beams, the acceleration length is limited by the fact that such pulses do not propagate without changing their transverse shape. Thus, any technique that allows for reaching some ion energy over shorter distance is bound to optimize the acceleration process.

Having established the improved performance of Eq. (8), we continue to discuss how a frequency chirp can be used to maintain the optimum condition Eq. (1). To this end, we require the reflection coefficient entering Eq. (4). A foil's reflection coefficient depends on the laser's and foil's parameters in its rest frame ($\gamma \approx 1$) according to[49]

$$\rho(\eta) = \frac{\epsilon_0(\eta)}{a_0(\eta)} \left(\frac{\left([\Delta^2 - 1]^2 + 4a_0^2\right)^{\frac{1}{2}} + \Delta^2 - 1}{\left([\Delta^2 - 1]^2 + 4a_0^2\right)^{\frac{1}{2}} + \Delta^2 + 1} \right)^{\frac{1}{2}}, \qquad (11)$$

where we defined the difference $\Delta^2(\eta) := a_0^2(\eta) - \epsilon_0^2(\eta)$. Transforming this relation back into the laboratory frame amounts to the replacement $\epsilon_0(\eta) \to \gamma(\eta)\epsilon_0(\eta)$. Hence, from Eq. (1) we read off that both in the foil's rest frame and the laboratory frame the optimum condition can be used to simplify the reflection coefficient. Consequently, in this work we can always use

$$\rho(\eta) = \left(\frac{(1 + 4a_0^2)^{\frac{1}{2}} - 1}{(1 + 4a_0^2)^{\frac{1}{2}} + 1} \right)^{\frac{1}{2}}. \qquad (12)$$

Assuming then properties of a typical foil of 10 nm thickness and a density of $n_e = 10^{23}$/cm^3, approximately corresponding to 50 times the critical density for an optical laser beam of 800 nm wavelength, driven by a laser with the above assumed Gaussian temporal profile and peak intensity $I = 10^{21}$ W/cm^2 we find a decisive dependency of the reflection coefficient on the incident frequency (see Fig. 2). We can also read off that this dependency is more pronounced the in the laser's rising edge where a_0 is lower, indicating that the laser frequency gives the finest tunability during the starting phase of RPA. Based on these results, it is apparent that even though Eq. (8) is formally
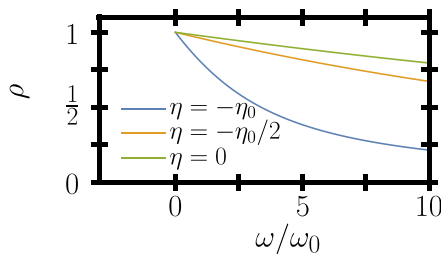
FIG. 2. Reflection coefficient as a function of the laser's frequency at various phases of the driving laser pulse for a foil of 10 nm thickness and a density of $n_e = 10^{23}/cm^3$ ($\approx 50\, n_{cr}\, [\omega_0 = 1.55\, eV]$).

independent of the laser's frequency, an appropriate pulse chirp can still be used to tailor the reflection coefficient and hence the overall acceleration. This approach is complementary to the tuning through an optimized intensity profile,[53] which is aimed in the ultra-relativistic regime. In contrast, the here presented frequency optimization is most apt to steer and stabilize the commonly highly unstable initial phase of radiation pressure acceleration. To find an optimal pulse chirp, a differential approach is favorable: Provided we can match the foil's momentum to its ideal value at a given time instant, from that time on the optimum condition can be enforced on its differential equation of motion (8). The optimum momentum, fulfilling Eq. (2) perpetually, on the other hand, changes as

$$\frac{dp^{opt}}{d\eta} = m_i \frac{\mathcal{E}'(\eta)\mathcal{E}(\eta)}{\sqrt{\mathcal{E}^2(\eta) - 1}}. \tag{13}$$

This differential change can be matched to Eq. (4) provided the reflection coefficient is given by

$$\rho(\eta) = \sqrt{\left(\frac{1}{\sqrt{\mathcal{E}^2(\eta) - 1}} + \frac{1}{\mathcal{E}(\eta)}\right)\frac{m_i \mathcal{E}'(\eta)}{|eE(\eta)|}}, \tag{14}$$

where we additionally assumed Eq. (8) to be fulfilled and the foil to be initially at rest $p(\eta_0) = 0$. Equating Eqs. (12) and (14) and solving for the laser frequency numerically will be a benchmark for our analytical results. We note that provided the optimal reflection coefficient (14) is maintained throughout the acceleration process, the foil ions' momentum will develop according to Eq. (13) and be given by Eq. (8). Additionally, we see that Eq. (14) is only meaningfully defined in the regime $\mathcal{E}'(\eta) \geq 0$, i.e., on the pulse's rising edge. This is physically due to the fact that according to Eq. (2) on the field envelope's decreasing edge a decreasing $\gamma(\eta)$ would be required to maintain the optimum condition, which would correspond to deceleration instead of the desired acceleration. We thus have to limit our analysis to the first half of the pulse, discriminated by $\mathcal{E}'(\eta) \geq 0$. We note that the results of Ref. 53 indicate that the optimal pulse profile has only the rising edge.

In accordance with the technical development we are going to consider high-intensity laser pulses defined by the condition $a_0 \gg 1$ and remind ourselves that the foil will be driven in a parameter regime close to the optimum condition (1), indicating that $a_0(\eta) \approx \gamma(\eta)\epsilon_0(\eta)$, where we did not yet assume Eq. (1) to

hold exactly. We can then study the acceleration process for the case of an ultra-relativistic foil $p_i \gg m_i$, as is common in investigations of the RPA scheme, and in addition in the foil's not commonly considered beginning, still non-relativistic acceleration phase $p_i \sim m_i$.

A. Non-relativistic foil motion

We begin studying the motion of a non-relativistic foil $1 - \gamma(\eta) \ll 1$, which, according to Eq. (2) translates to the condition $|\mathcal{E}(\eta)| \sim 1$. From Eq. (1), we deduce that in this case close to the optimum drive regime the foil's and laser's parameters are linked by $\epsilon_0 \approx a_0$. Furthermore, from Eq. (9) we see that in the regime $\mathcal{E} \sim 1$ the acceleration will be confined to phases $\eta_0 \ll \tau_L$, such that the field will not be strongly changing $\mathcal{E}'(\eta) \ll \mathcal{E}(0)/\tau_L$. From Eq. (14) we thus see that the optimal reflection coefficient has to be rather small, which is achievable for large laser frequencies (compare Fig. 2). This in turn, however, implies small values of a_0, even for high laser powers. In order to corroborate this conjecture, we need to find an analytical expression for the laser's frequency structure ensuring that the foil's reflection coefficient from Eq. (12) is matched to its optimal reflection derived in Eq. (14). To find such a solution for the optimized laser frequency, we again solve the foil's equation of motion (4) through separation of variables and find that, when neglecting absorption in the foil, in the non-relativistic regime the momentum of a foil initially at rest is given by

$$p_0(\eta) = \int_{\eta_0}^{\eta} d\eta' \frac{|\rho(\eta')eE(\eta')|^2}{eE_{foil}}. \tag{15}$$

The same result can be found expanding solution (5) to the lowest order in p_0/m_i. From Eq. (8), we deduce that the phase dependent reflection coefficient required to meet the optimum condition is given by

$$\rho(\eta) = \sqrt{\frac{m_i \mathcal{E}'(\eta)}{|eE(\eta)|\sqrt{\mathcal{E}^2(\eta) - 1}}}, \tag{16}$$

which is equivalent to approximating the solution of Eq. (14) in the regime $\sqrt{\mathcal{E}^2(\eta) - 1} \ll \mathcal{E}(\eta)$. Equating this to the approximation (12), we find that an appropriate laser frequency chirp can ensure condition (1) to be satisfied in the regime $\mathcal{E} \sim 1$, provided that it holds

$$\omega_{NR}^{opt}(\eta) = \frac{eE(\eta)}{m_e}\left(\frac{|eE(\eta)|\sqrt{\mathcal{E}^2(\eta) - 1} - m_i \mathcal{E}'(\eta)}{\sqrt{m_i \mathcal{E}'(\eta)|eE(\eta)|\sqrt{\mathcal{E}^2(\eta) - 1}}}\right). \tag{17}$$

Comparing this analytical expression to the numerically consistent solution of Eqs. (12) and (14) for a foil of 10 μm thickness and $n_e = 9 \times 10^{23}\, cm^3 \approx 520\, n_{crit}$ accelerated by a laser pulse of intensity $I = 10^{21}\, W/cm^2$ and $\tau_L = 10^3/\omega_0$ we find good agreement with the outlined derivation (see Fig. 3). We also find our conjecture confirmed that the required laser frequencies are several hundreds of eV, as issued above.
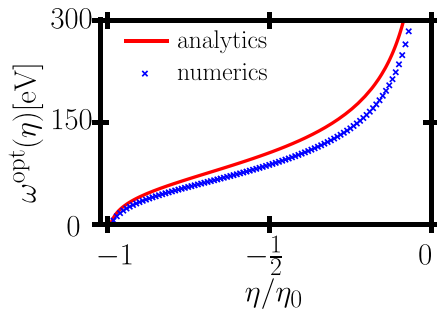
FIG. 3. Optimal laser frequency in the non-relativistic model case (parameters in the text) according to the analytical solution equation (17) (solid red) in comparison to the numerical solution of equations (12) and (14) (blue crosses).

B. Ultra-relativistic foil motion

We now turn to studying the motion of an ultra-relativistic foil $\gamma(\eta) \gg 1$, which, according to Eq. (2) translates to the condition $|\mathcal{E}(\eta)| \gg 1$. In this regime, as can be deduced from Eq. (9) we see that the acceleration will be occurring over the whole phase interval $\eta \in [-\tau_L, \tau_L]$. Consequently, in contrast to the previously studied non-relativistic case, the field's derivative can be estimated to be of the order $\mathcal{E}'(\eta) \sim \mathcal{E}(\eta)/\tau_L$. Hence, we can estimate from Eq. (14) that in this regime the optimal reflection coefficient will be of the order $\rho \lesssim \sqrt{2m_i/|eE(\eta)|\tau_L}$. This indicates that for ultra-relativistic foil motion in the pulse center, i.e., for largest field strengths, the optimally matched reflection coefficient again has to be small, which in the present scheme is achievable by large frequencies. On the other hand, from Eq. (12) one infers that the maximal reflection coefficient $\rho \to 1$ is reached for $a_0 \to \infty$, corresponding to the low-frequency limit $\omega \to 0$. As a result, in the beginning phase of the acceleration the reflection coefficient can still be small, facilitating the use of optical laser frequencies. From this result, however, we infer a further restriction: The optimum condition (2) can only be maintained up to the phase instant, where the value of the required optimally matched reflection coefficient from Eq. (14) exceeds the maximum achievable value ρ_{max}. This phase instant is implicitly defined by the condition

$$\mathcal{E}'(\eta) \leq \frac{|eE_{foil}|}{2m_i}. \tag{18}$$

Assuming again the Gaussian field shape $E(\eta) = E_{max} \exp[-2\log(2)(\eta/\tau_L)^2]$, in the pulse's rising edge the scaled field's derivative is maximal at the phase instant $\tilde{\eta} = -\tau_L/2\sqrt{\log(2)}$, whence for the specified pulse shape we can rewrite Eq. (18) as a maximal condition for the pulse duration in the form

$$\tau_L \geq \frac{4m_i\sqrt{\log(2)}}{|eE_{foil}|}\mathcal{E}_{max}e^{-\frac{1}{2}}, \tag{19}$$

which ensures that the optimally matched reflection coefficient can always be matched by Eq. (12). Since we fix the intensity profile, the change in laser frequency leads to a_0 changing its value accordingly by a couple of orders of magnitude. Consequently, for ultra-relativistic foil motion, the matching between Eq. (12)

and the foil's optimal reflection coefficient Eq. (14) requires to again solve Eq. (4) by separating the variables and integration. The result is formally the same expression for the foil's momentum as in the non-relativistic case but, from Eq. (8) we deduce that in the case $\gamma \gg 1$ the phase dependent reflection coefficient required to meet condition (13) is given by

$$\rho(\eta) = \sqrt{\frac{2m_iE'(\eta)}{eE^2(\eta)}}, \tag{20}$$

which is equivalent to approximating Eq. (14) in the regime $\mathcal{E}(\eta) \gg 1$. Equating this to the approximation (12) we arrive at an equation which is very similar to the one obtained in the non-relativistic case. We find the appropriate laser frequency chirp, ensuring condition (1) to be satisfied in the regime $\gamma \gg 1$ to be given by

$$\omega_{UR}^{opt}(\eta) = \frac{eE(\eta)}{m_e}\left(\frac{|eE^2(\eta)| - 2m_iE'(\eta)}{\sqrt{2m_iE'(\eta)|eE^2(\eta)|}}\right). \tag{21}$$

By virtue of the condition $\mathcal{E}(\eta) \leq 1$ established subsequent to Eq. (8), we can rewrite condition (18) to read $2m_iE'(\eta) \leq |eE^2(\eta)|$ and conclude that latter condition (18) to be required for $\omega_{UR}^{opt}(\eta)$ to have positive, i.e., physical solutions. We can hence interpret that condition as the physical prerequisite of the optimally matched reflection coefficient to be reachable through tuning the frequency. Comparing the analytical expression (21) to the numerically consistent solution of Eqs. (12) and (14) for a foil of 1 nm thickness and density $n_e = 10^{23}$ cm$^3 \approx 60\,n_{crit}$ accelerated by a laser pulse of intensity $I = 10^{19}$ W/cm^2 and duration $\tau_L = 3 \times 10^4/\omega_0$ we find our analytical approximation very well confirmed (see Fig. 4). We also find the required laser frequencies to lie in significantly lower energy ranges as compared to the non-relativistic case. This behavior can be explained by the observation that the equality between Eqs. (12) and (20) in the regime $\mathcal{E}(\eta) \gg 1$ is achieved for larger values of a_0 than the equality between Eqs. (12) and (16) in the regime $\mathcal{E}(\eta) \sim 1$. Physically, this translates to the observation that an ultra-relativistic foil can withstand stronger laser acceleration, as experienced in lower frequency fields. Also the divergence of the optimum frequencies for later phases $\eta \to 0$ is readily explainable as the field derivative $E'(\eta)$ goes to zero in this regime, indicating that the
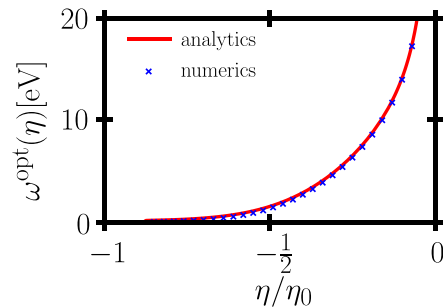
FIG. 4. Optimal laser frequency in the ultra-relativistic model case (parameters in the text) according to the analytical solution equation (21) (solid red) in comparison to the numerical solution of equations (12) and (14) (blue crosses).

optimum reflection coefficient (20) vanishes as well, which is achieved for very large frequencies, only. We furthermore note that at the time instant $\eta = 0$ in the above example the foil has already been accelerated to $\gamma(\eta = 0) = \mathcal{E}(\eta = 0) \sim 10$, while constantly maintaining the optimum condition (1). This example indicates that indeed the suggested method is also applicable to ultra-relativistic foil motion, provided one can supply the required high-frequency photon beams.

III. CONCLUSION

In summary, we have presented a systematic study of how an appropriately chosen frequency chirp serves to maintain an optimum condition in the radiation pressure acceleration of a thin foil. We presented analytical expressions for the required pulse chirp in two limiting cases of nonrelativistic as well as ultra-relativistic foil motion. Comparing these limiting cases to exact numerical solutions of the defining equations of the pulse's frequency structure required to maintain optimal acceleration conditions, we found excellent agreement between the exact and approximate solutions. As a caveat, it has to be noted that the found optimal frequency chirps stretch to high frequencies of 10s and 100s of eV (corresponding to wavelengths of $\mathcal{O}(10)$ nm and $\mathcal{O}(1)$ nm, respectively) in the regime of ultra-relativistic and nonrelativistic foil motion, respectively. Such high-energy beams, however, are beyond the capabilities provided by high-power laser facilities available today[3–7] or expected to become operational within short time.[8,9] To overcome this shortcoming, there are several routes conceptually imaginable, such as technological development, e.g., of free electron lasers,[58–60] or frequency up-conversion techniques in the ultra-high intensity regime. On the other hand, even though the required frequency distributions are not yet feasible, the conceptual analysis presented here may still prove useful for an improved understanding of the overall acceleration process and guidance for future laser developments.

REFERENCES

[1] S. Busold, A. Almomani, V. Bagnoud, W. Barth, S. Bedacht, A. Blažević, O. Boine-Frankenheim, C. Brabetz, T. Burris-Mog, T. Cowan, O. Deppert, M. Droba, H. Eickhoff, U. Eisenbarth, K. Harres, G. Hoffmeister, I. Hofmann, O. Jaeckel, R. Jaeger, M. Joost, S. Kraft, F. Kroll, M. Kaluza, O. Kester, Z. Lecz, T. Merz, F. Nürnberg, H. Al-Omari, A. Orzhekhovskaya, G. Paulus, J. Polz, U. Ratzinger, M. Roth, G. Schaumann, P. Schmidt, U. Schramm, G. Schreiber, D. Schumacher, T. Stoehlker, A. Tauschwitz, W. Vinzenz, F. Wagner, S. Yaramyshev, and B. Zielbauer, Nucl. Instrum. Methods Phys. Res., Sect. A **740**, 94 (2014).

[2] F. Mackenroth, A. Gonoskov, and M. Marklund, Eur. Phys. J. D **71**, 204 (2017).

[3] C. Danson, D. Hillier, N. Hopps, and D. Neely, High Power Laser Sci. Eng. **3**, e3 (2015).

[4] C. Danson, P. Brummitt, R. Clarke, J. Collier, B. Fell, A. Frackiewicz, S. Hancock, S. Hawkes, C. Hernandez-Gomez, P. Holligan, M. Hutchinson, A. Kidd, W. Lester, I. Musgrave, D. Neely, D. Neville, P. Norreys, D. Pepler, C. Reason, W. Shaikh, T. Winstone, R. Wyatt, and B. Wyborn, Nucl. Fusion **44**, S239 (2004).

[5] C. J. Hooker, J. L. Collier, O. Chekhlov, R. Clarke, E. Divall, K. Ertel, B. Fell, P. Foster, S. Hancock, A. Langley, D. Neely, J. Smith, and B. Wyborn, J. Phys. IV France **133**, 673 (2006).

[6] K. Nakamura, H. S. Mao, A. J. Gonsalves, H. Vincenti, D. E. Mittelberger, J. Daniels, A. Magana, C. Toth, and W. P. Leemans, IEEE J. Quantum Electron. **53**, 1 (2017).

[7] See https://www.ibs.re.kr/eng/sub02_03_05.do for CORELS.

[8] *Extreme Light Infrastructure – Whitebook*, edited by G. A. Mourou, G. Korn, W. Sandner, and J. L. Collier (Andreas Thoss, 2011).

[9] S. Gales, K. A. Tanaka, D. L. Balabanski, F. Negoita, D. Stutman, O. Tesileanu, C. A. Ur, D. Ursescu, I. Andrei, S. Ataman, M. O. Cernaianu, L. DAlessi, I. Dancus, B. Diaconescu, N. Djourelov, D. Filipescu, P. Ghenuche, D. G. Ghita, C. Matei, K. Seto, M. Zeng, and N. V. Zamfir, Rep. Prog. Phys. **81**, 094301 (2018).

[10] Z. Major, S. A. Trushin, I. Ahmad, M. Siebold, C. Wandt, S. Klingebiel, T.-J. Wang, J. A. F. Lop, A. Henig, S. Kruber, R. Weingartner, A. Popp, J. Osterhoff, R. Hörlein, J. Hein, V. Pervak, A. Apolonski, F. Krausz, and S. Karsch, Rev. Laser Eng. **37**, 431 (2009).

[11] J. Zou, C. L. Blanc, D. Papadopoulos, G. Chriaux, P. Georges, G. Mennerat, F. Druon, L. Lecherbourg, A. Pellegrina, P. Ramirez et al., High Power Laser Sci. Eng. **3**, e2 (2015).

[12] J. Kawanaka, K. Tsubakimoto, H. Yoshida, K. Fujioka, Y. Fujimoto, S. Tokita, T. Jitsuno, N. Miyanaga, and G.-E. D. Team, J. Phys.: Conf. Ser. **688**, 012044 (2016).

[13] See http://www.xcels.iapras.ru/ for XCELS.

[14] G. A. Mourou, T. Tajima, and S. V. Bulanov, Rev. Mod. Phys. **78**, 309 (2006).

[15] H. Daido, M. Nishiuchi, and A. S. Pirozhkov, Rep. Prog. Phys. **75**, 056401 (2012).

[16] A. Macchi, M. Borghesi, and M. Passoni, Rev. Mod. Phys. **85**, 751 (2013).

[17] S. V. Bulanov, J. J. Wilkens, T. Z. Esirkepov, G. Korn, G. Kraft, S. D. Kraft, M. Molls, and V. S. Khoroshkov, Phys.-Usp. **57**, 1149 (2014).

[18] S. C. Wilks, A. B. Langdon, T. E. Cowan, M. Roth, M. Singh, S. Hatchett, M. H. Key, D. Pennington, A. MacKinnon, and R. A. Snavely, Phys. Plasmas **8**, 542 (2001).

[19] M. Roth, A. Blazevic, M. Geissel, T. Schlegel, T. Cowan, M. Allen, J. Gauthier, P. Audebert, J. Fuchs, J. Meyer-ter Vehn, M. Hegelich, S. Karsch, and A. Pukhov, Phys. Rev. Spec. Top. Accel. Beams **5**, 061301 (2002).

[20] P. Mora, Phys. Rev. Lett. **90**, 185002 (2003).

[21] T. E. Cowan, J. Fuchs, H. Ruhl, A. Kemp, P. Audebert, M. Roth, R. Stephens, I. Barton, A. Blazevic, E. Brambrink, J. Cobble, J. Fernández, J.-C. Gauthier, M. Geissel, M. Hegelich, J. Kaae, S. Karsch, G. P. Le Sage, S. Letzring, M. Manclossi, S. Meyroneinc, A. Newkirk, H. Pépin, and N. Renard-LeGalloudec, Phys. Rev. Lett. **92**, 204801 (2004).

[22] M. Passoni, L. Bertagna, and A. Zani, New J. Phys. **12**, 045012 (2010).

[23] T. Esirkepov, S. Bulanov, K. Nishihara, T. Tajima, F. Pegoraro, V. Khoroshkov, K. Mima, H. Daido, Y. Kato, Y. Kitagawa, K. Nagai, and S. Sakabe, Phys. Rev. Lett. **89**, 175003 (2002).

[24] I. Last, I. Schek, and J. Jortner, J. Chem. Phys. **107**, 6685 (1997).

[25] S. Bulanov, T. Esirkepov, V. Khoroshkov, A. Kuznetsov, and F. Pegoraro, Phys. Lett. A **299**, 240 (2002).

[26] V. F. Kovalev and V. Y. Bychenkov, Phys. Rev. Lett. **90**, 185004 (2003).

[27] E. Fourkal, I. Velchev, and C.-M. Ma, Phys. Rev. E **71**, 036412 (2005).

[28] I. Last and J. Jortner, Proc. Natl. Acad. Sci. U.S.A. **102**, 1291 (2005).

[29] M. Murakami and M. M. Basko, Phys. Plasmas **13**, 012105 (2006).

[30] S. C. Wilks, W. L. Kruer, M. Tabak, and A. B. Langdon, Phys. Rev. Lett. **69**, 1383 (1992).

[31] N. Naumova, T. Schlegel, V. T. Tikhonchuk, C. Labaune, I. V. Sokolov, and G. Mourou, Phys. Rev. Lett. **102**, 025002 (2009).

[32] S. Palaniyappan, B. M. Hegelich, H.-C. Wu, D. Jung, D. C. Gautier, L. Yin, B. J. Albright, R. P. Johnson, T. Shimada, S. Letzring, D. T. Offermann, J. Ren, C. Huang, R. Hrlein, B. Dromey, J. C. Fernandez, and R. C. Shah, Nat. Phys. **8**, 763 (2012).

[33]B. M. Hegelich, I. Pomerantz, L. Yin, H. C. Wu, D. Jung, B. J. Albright, D. C. Gautier, S. Letzring, S. Palaniyappan, R. Shah, K. Allinger, R. Hörlein, J. Schreiber, D. Habs, J. Blakeney, G. Dyer, L. Fuller, E. Gaul, E. Mccary, A. R. Meadows, C. Wang, T. Ditmire, and J. C. Fernandez, New J. Phys. **15**, 085015 (2013).

[34]D. Jung, B. J. Albright, L. Yin, D. C. Gautier, R. Shah, S. Palaniyappan, S. Letzring, B. Dromey, H.-C. Wu, T. Shimada, R. P. Johnson, M. Roth, J. C. Fernandez, D. Habs, and B. M. Hegelich, New J. Phys. **15**, 123035 (2013).

[35]D. Haberberger, S. Tochitsky, F. Fiuza, C. Gong, R. A. Fonseca, L. O. Silva, W. B. Mori, and C. Joshi, Nat. Phys. **8**, 95 (2012).

[36]A. V. Kuznetsov, T. Z. Esirkepov, F. F. Kamenets, and S. V. Bulanov, Plasma Phys. Rep. **27**, 211 (2001).

[37]S. V. Bulanov and T. Z. Esirkepov, Phys. Rev. Lett. **98**, 049503 (2007).

[38]F. Mackenroth, A. Gonoskov, and M. Marklund, Phys. Rev. Lett. **117**, 104801 (2016).

[39]J. Magnusson, F. Mackenroth, M. Marklund, and A. Gonoskov, Phys. Plasmas **25**, 053109 (2018).

[40]T. Esirkepov, M. Borghesi, S. V. Bulanov, G. Mourou, and T. Tajima, Phys. Rev. Lett. **92**, 175003 (2004).

[41]S. V. Bulanov, E. Y. Echkina, T. Z. Esirkepov, I. N. Inovenkov, M. Kando, F. Pegoraro, and G. Korn, Phys. Rev. Lett. **104**, 135003 (2010).

[42]A. Henig, S. Steinke, M. Schnuerer, T. Sokollik, R. Hoerlein, D. Kiefer, D. Jung, J. Schreiber, B. M. Hegelich, X. Q. Yan, J. Meyer-ter Vehn, T. Tajima, P. V. Nickles, W. Sandner, and D. Habs, Phys. Rev. Lett. **103**, 245003 (2009).

[43]S. Kar, K. F. Kakolee, B. Qiao, A. Macchi, M. Cerchez, D. Doria, M. Geissler, P. McKenna, D. Neely, R. Prasad, R. Quinn, B. Ramakrishna, G. Sarri, M. Willi, X. Y. Yuan, M. Zepf, and M. Borghesi, Phys. Rev. Lett. **109**, 185006 (2012).

[44]F. Pegoraro and S. V. Bulanov, Phys. Rev. Lett. **99**, 065002 (2007).

[45]S. S. Bulanov, E. Esarey, C. B. Schroeder, S. V. Bulanov, T. Z. Esirkepov, M. Kando, F. Pegoraro, and W. P. Leemans, Phys. Rev. Lett. **114**, 105003 (2015).

[46]S. S. Bulanov, E. Esarey, C. B. Schroeder, S. V. Bulanov, T. Z. Esirkepov, M. Kando, F. Pegoraro, and W. P. Leemans, Phys. Plasmas **23**, 056703 (2016).

[47]I. J. Kim, K. H. Pae, I. W. Choi, C.-L. Lee, H. T. Kim, H. Singhal, J. H. Sung, S. K. Lee, H. W. Lee, P. V. Nickles, T. M. Jeong, C. M. Kim, and C. H. Nam, Phys. Plasmas **23**, 070701 (2016).

[48]A. Higginson, R. J. Gray, M. King, R. J. Dance, S. D. R. Williamson, N. M. H. Butler, R. Wilson, R. Capdessus, C. Armstrong, J. S. Green, S. J. Hawkes, P. Martin, W. Q. Wei, S. R. Mirfayzi, X. H. Yuan, S. Kar, M. Borghesi, R. J. Clarke, D. Neely, and P. McKenna, Nat. Commun. **9**, 724 (2018).

[49]V. A. Vshivkov, N. M. Naumova, F. Pegoraro, and S. V. Bulanov, Phys. Plasmas **5**, 2727 (1998).

[50]A. Macchi, S. Veghini, and F. Pegoraro, Phys. Rev. Lett. **103**, 085003 (2009).

[51]A. Macchi, S. Veghini, T. V. Liseykina, and F. Pegoraro, New J. Phys. **12**, 045013 (2010).

[52]A. Sgattoni, P. Londrillo, A. Macchi, and M. Passoni, Phys. Rev. E **85**, 036405 (2012).

[53]S. S. Bulanov, C. B. Schroeder, E. Esarey, and W. P. Leemans, Phys. Plasmas **19**, 093112 (2012).

[54]J.-X. Li, Y. I. Salamin, B. J. Galow, and C. H. Keitel, Phys. Rev. A **85**, 063832 (2012).

[55]J.-L. Liu, Z. M. Sheng, J. Zheng, C. S. Liu, and J. Zhang, Phys. Rev. Spec. Top. Accel. Beams **15**, 041301 (2012).

[56]A. A. Sahai, T. Katsouleas, R. Bingham, W. Mori, A. Tableman, F. Tsung, and M. Tzoufras, in Proceedings of IPAC (2012), Vol. T25, p. 2654.

[57]H. Vosoughian, Z. Riazi, H. Afarideh, and E. Yazdani, Phys. Plasmas **22**, 073110 (2015).

[58]B. W. J. McNeil and N. R. Thompson, Nat. Photonics **4**, 814 (2010).

[59]M. Altarelli, Nucl. Instrum. Methods Phys. Res., Sect. B **269**, 2845 (2011).

[60]R. Abela, A. Aghababyan, M. Altarelli, C. Altucci, G. Amatuni, P. Anfinrud, P. Audebert, V. Ayvazyan, N. Baboi, J. Baehr, V. Balandin, R. Bandelmann, J. Becker, B. Beutner, C. Blome, I. Bohnet, A. Bolzmann, C. Bostedt, Y. Bozhko, A. Brandt, S. Bratos, C. Bressler, O. Brovko, H. Brck, J. P. Carneiro, S. Casalbuoni, M. Castellano, P. Castro, L. Catani, A. Cavalleri, S. Celik, H. Chapman, D. Charalambidis, J. Chen, M. Chergui, S. Choroba, A. Cianchi, M. Clausen, E. Collet, H. Danared, C. David, W. Decking, M. Dehler, H. Delsim-Hashemi, G. Dipirro, B. Dobson, M. Dohlus, S. Duesterer, A. Eckhardt, H. J. Eckoldt, H. Edwards, B. Faatz, M. Fajardo, A. Fateev, J. Feldhaus, Y. Filipov, K. Floettmann, R. Follath, B. Fominykh, M. French, J. Frisch, L. Froehlich, E. Gadwinkel, L. Garca-Tabars, J. J. Gareta, T. Garvey, F. Gel'mukhanov, U. Gensch, C. Gerth, M. Goerler, N. Golubeva, H. Graafsma, W. Graeff, O. Grimm, B. Griogoryan, G. Grbel, C. Gutt, K. Hacker, L. Haenisch, U. Hahn, J. Hajdu, J. H. Han, M. Hartrott, J. Havlicek, O. Hensler, K. Honkavaara, V. Honkimki, T. Hott, M. R. Howells, M. Huening, H. Ihee, F. Ilday, R. Ischebeck, M. Jablonka, E. Jaeschke, K. Jensch, J. P. Jensen, S. Johnson, L. Juha, F. Kaerntner, R. Kammering, H. Kapitza, V. Katalev, B. Keil, S. Khodyachykh, R. Kienberger, J. W. Kim, Y. Kim, K. Klose, V. Kocharyan, W. Koehler, M. Koerfer, M. Kollewe, Q. Kong, W. Kook, D. Kostin, O. Kozlov, D. Kraemer, M. Krasilnikov, B. Krause, O. Krebs, J. Krzywinski, G. Kube, M. Kuhlmann, H. Laich, R. Lange, M. Larsson, R. W. Lee, A. Leuschner, H. Lierl, L. Lilje, T. Limberg, A. Lindenberg, D. Lipka, F. Loehl, K. Ludwig, M. Luong, C. Magne, A. Maquet, J. Marangos, C. Masciovecchio, M. Maslov, A. Matheisen, E. Matyushevskiy, O. Matzen, H. J. May, I. McNulty, D. McCormick, P. Meulen, N. Meyners, P. Michelato, N. Mildner, V. Miltchev, M. Minty, W. D. Moeller, T. Mller, L. Monaco, M. Nagl, O. Napoly, G. Neubauer, P. Nicolosi, A. Nienhaus, D. Noelle, T. Nunez, F. Obier, A. Oppelt, C. Pagani, R. Paparella, H. B. Pedersen, B. Petersen, R. Petrosyan, L. Petrosyan, A. Petrov, P. Piot, J. Pflueger, A. Plech, E. Ploenjes, L. Poletto, G. Pplau, E. Prat, S. Prat, J. Prenting, D. Proch, D. Pugachov, H. Quack, B. Racky, D. Ramert, H. Redlin, K. Rehlich, R. Reininger, H. Remde, D. Reschke, D. Richter, M. Richter, S. Riemann, D. Riley, I. Robinson, J. Roensch, F. Rosmej, M. Ross, J. Rossbach, V. Rybnikov, M. Sachwitz, E. Saldin, W. Sandner, J. Schfer, T. Schilcher, H. Schlarb, M. Schloesser, V. Schlott, B. Schmidt, M. Schmitz, P. Schmueser, J. Schneider, E. Schneidmiller, F. Schotte, S. Schrader, S. Schreiber, C. Schroer, R. Schuch, H. Schulte-Schrepping, A. Schwarz, M. Seidel, J. Sekutowicz, P. Seller, D. Sellmann, F. Senf, D. Sertore, A. Shabunov, S. Simrock, W. Singer, H. Sinn, R. Smith, E. Sombrowski, A. A. Sorokin, E. Springate, M. Staack, L. Staykov, B. Steffen, B. Stephenson, F. Stephan, F. Stulle, E. Syresin, K. Sytchev, V. Sytchev, G. Tallents, S. Techert, N. Tesch, H. Thom, K. Tiedtke, M. Tischer, M. Tolan, S. Toleikis, F. Toral, R. Treusch, D. Trines, V. Tsakanov, I. Tsakov, T. Tschentscher, F. R. Ullrich, U. van Rienen, A. Variola, I. Vartaniants, E. Vogel, J. Vogel, R. Vuilleumier, H. Wabnitz, R. Wanzenberg, J. S. Wark, H. Weddig, T. Weiland, H. Weise, M. Wendt, R. Wenndorff, R. Wichmann, I. Will, A. Winter, K. Witte, K. Wittenburg, P. Wochner, T. Wohlenberg, J. Wojtkiewicz, A. Wolf, M. Wulff, M. Yurkov, I. Zagorodnov, P. Zambolin, K. Zapfe, P. Zeitoun, V. Ziemann, A. Zolotov, R. Brinkmann, and H. J. Grabosch, "XFEL: The European X-Ray Free-Electron Laser – Technical Design Report," Report No. DESY 2006-097 (DESY, Hamburg, 2006), pp. 1–646.